

Referring Video Object Segmentation with Inter-Frame Interaction and Cross-Modal Correlation

Meng Lan
Wuhan University
menglan@whu.edu.cn

Fu Rong
Wuhan University
furong@whu.edu.cn

Lefei Zhang
Wuhan University
zhanglefei@whu.edu.cn

Abstract

Referring video object segmentation (RVOS) aims to segment the target object in a video sequence described by a language expression. Typical query-based methods process the video sequence in a frame-independent manner to reduce the high computational cost, which however affects the performance due to the lack of inter-frame interaction for temporal coherence modeling and spatio-temporal representation learning of the referred object. Besides, they directly adopt the raw and high-level sentence feature as the language queries to decode the visual features, where the weak correlation between visual and linguistic features also increases the difficulty of decoding the target information and limits the performance of the model. In this paper, we propose a novel RVOS framework, dubbed IFIRVOS, to address these issues. Specifically, we design a plug-and-play inter-frame interaction module in the Transformer decoder to efficiently learn the spatio-temporal features of the referred object, so as to decode the object information in the video sequence more precisely and generate more accurate segmentation results. Moreover, we devise the vision-language interaction module before the multimodal Transformer to enhance the correlation between the visual and linguistic features, thus facilitating the process of decoding object information from visual features by language queries in Transformer decoder and improving the segmentation performance. Extensive experimental results on three benchmarks validate the superiority of our IFIRVOS over state-of-the-art methods and the effectiveness of our proposed modules.

1. Introduction

Referring video object segmentation aims to segment the target object in a video sequence described by a language expression [28]. This emerging multimodal task has attracted great attention in the research community since it provides a more natural way for human-computer in-

teraction. RVOS has a wide range of applications, *e.g.*, language-based video editing and surveillance. Compared with the semi-supervised video object segmentation task [21], which relies on the mask annotations in the first frame, RVOS is more challenging due to the diversity of language expressions and the difficulties in exploiting the cross-modal knowledge.

Various RVOS datasets and approaches have been proposed in the development of the field. For example, Khoreva *et al.* [12] establishes a new benchmark for RVOS by augmenting the popular VOS benchmarks, *e.g.*, DAVIS2016 [25] and DAVIS2017 [26], with language descriptions. A baseline method is provided by combining the referring expression grounding model [40] and the segmentation model. URVOS [28] constructs the first large-scale RVOS dataset called Refer-Youtube-VOS by annotating the referring expressions for the Youtube-VOS dataset [37]. Recently, the multimodal Transformer based RVOS methods [2,35] are drawing increasing attention for their impressive performance. They model RVOS as a sequence prediction task and extend the DETR architecture [3] to make predictions for all possible objects in the video sequence prior to selecting the one that matches the language description. Among them, ReferFormer [35] takes the language description as the query of the multimodal Transformer and produces the target-aware instance embeddings for the instance sequence prediction, which achieves the state-of-the-art performance.

Although the language queries based method has demonstrated its impressive performance on several benchmarks, ReferFormer still has two limitations, as shown in Fig.1 (a). First, to avoid high computational cost, ReferFormer chooses to query the video sequence in a frame-independent manner, which however may lead to performance degradation since there is a lack of inter-frame interaction to accomplish the modeling of temporal coherence and the learning of spatio-temporal representation for the referred object. Second, ReferFormer directly adopts the raw and high-level sentence feature without any interaction with visual features as the language queries to decode the image fea-

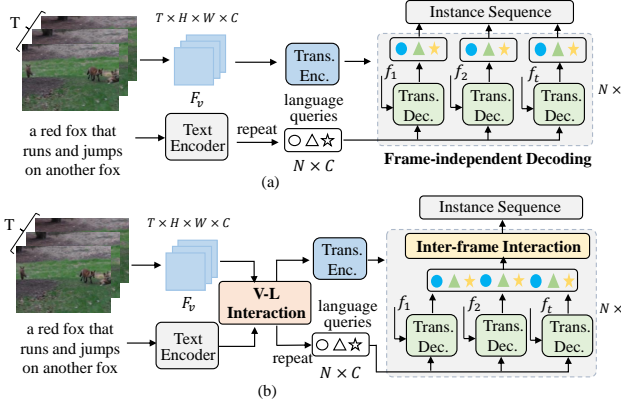


Figure 1. Comparison of previous language queries based RVOS method and our proposed IFIRVOS. (a) ReferFormer, (b) IFIRVOS

tures, and we argue that the weak correlation between visual and linguistic features before multimodal Transformer also increases the difficulty of decoding the object information accurately and limits the further improvement of model performance. Therefore, how to efficiently learn the spatio-temporal representation of the target object and enhance the correlation between the linguistic and visual features before the Transformer decoder is crucial to improve the object segmentation performance of the language queries based model.

In this paper, we propose a novel language queries based RVOS framework dubbed IFIRVOS to address the above-mentioned issues, as shown in Fig.1 (b). First, based on the multimodal Transformer architecture, we design a plug-and-play *inter-frame interaction module* for the Transformer decoder to efficiently model the temporal coherence and learn the spatio-temporal representation of the referred object. Specifically, an inter-frame interaction layer is inserted behind each decoder layer of the Transformer, in which the instance embeddings generated by the frame-independent decoding process are first unfolded in the spatio-temporal dimension, and then the inter-frame global correlation and spatio-temporal representation of the queried object are learned through the self-attention mechanism. The instance embeddings output from the inter-frame interaction layer are transformed back into the frame-independent state, and then fed into the next decoder layer or directly as the output of the decoder. In this manner, the multimodal Transformer could decode the object information in the video sequence more precisely and predict more accurate segmentation results.

Besides, we devise a *vision-language interaction module* before the multimodal Transformer to reinforce the cross-modal correlation between the visual and linguistic features, thus facilitating the process of decoding object informa-

tion from visual features by language queries in the Transformer decoder. Concretely, the vision-language interaction module maintains two parallel submodules that use the cross-modal features to enhance visual features and linguistic features, respectively. The strong correlation between the cross-modal features could ease of the language queries based cross-modal decoding process and promote the model to decode more accurate instance embedding, thereby improving the segmentation performance of the model.

Empirical results on several benchmark datasets demonstrate that these two simple and effective modules can significantly improve the RVOS performance compared with the baseline model. The main contributions of this work can be summarized as follows:

- We propose a novel RVOS framework dubbed IFIRVOS, which aims to efficiently decode precise and consistent instance embeddings from video sequence by learning the spatio-temporal target representation and enhancing the correlation between the cross-modal features. IFIRVOS outperforms the previous cutting-edge methods on several benchmarks and realizes the state-of-the-art performance.
- We design the inter-frame interaction module in the Transformer decoder to efficiently model the temporal coherence and learn the spatio-temporal representation of the queried object, so as to decode more accurate instance embeddings for predicting high-quality segmentation results.
- We devise the vision-language interaction module before the multimodal Transformer to boost the correlation between the cross-modal features, thus facilitating the decoding process of target information in the Transformer decoder and further improving the model performance.

2. Related work

Referring Video Object Segmentation. RVOS is a more challenging cross-modal task since it only uses the language description rather than the mask as the object reference. RVOS can be regarded as an extension of referring image segmentation (RIS) [33] by extending the input from the image domain to the video domain. Therefore, an intuitive RVOS method is applying the RIS methods on the video frames independently, e.g., RefVOS [1]. However, such an approach fails to consider the temporal information across frames, leading to inconsistent target predictions due to the scene and object appearance variations. To solve this problem, URVOS [28] treats this task as a joint problem of RIS in an image and mask propagation in a video, and proposes a united framework that maintains a

memory attention module to propagate the target information to the current frame. To learn a more effective target representation, VTCapsule [23] encodes each modality in capsules while ACGA [31] designs an asymmetric cross-guided attention network to enhance the linguistic and visual features. For achieving an accurate spatial-temporal consistency of the referred object, [6] proposes to utilize language as an intermediary bridge to accomplish explicit and adaptive spatial-temporal interaction. [34] integrates multi-level target features to enable more effective vision-language semantic alignment. Inspired by the success of the query-based Transformer frameworks in other fields [3,32], query-based multimodal Transformers are also explored in the RVOS task. MTTR [2] models the RVOS task as a sequence prediction problem and processes the video and text together in a multimodal Transformer. ReferFormer [35] follows this idea while using the sentence feature as the queries to find the referred object.

Video Instance Segmentation. Video Instance Segmentation (VIS) [27] could provide inspiration for RVOS task, since VIS intends to segment all seen objects and RVOS can be regarded as a special case of it, *i.e.*, segmenting referred object. DETR [3] is a widely used architecture in object detection field, which uses a set of object queries to infer the global context of the image and the relationships between the objects, and then outputs a set of predicted sequences in parallel. The idea is also introduced to the VIS task. VisTR [32] introduces the DETR model to VIS by treating the VIS as an end-to-end parallel sequence prediction problem and using parallel sequence decoding to solve it. However, VisTR integrates the spatio-temporal dimension of the video features and feeds them directly into the Transformer, resulting in a huge computational burden. To solve this problem, IFC [11] proposes the inter-frame communication Transformers, which incorporates memory tokens in the Transformer encoder to reduce the overhead of spatio-temporal information transfer. VITA [9] uses the mask2former model [4] to distill object-specific contexts into object tokens, and then accomplishes video-level understanding by associating frame-level object tokens. Inspired by these approaches in learning the spatio-temporal representation of the objects, we propose a new inter-frame interaction mechanism for RVOS task that directly performs the inter-frame interactions on candidate objects of different frames during the decoding process of the Transformer decoder. This strategy makes the inter-frame interaction between the instance embeddings for each frame more efficient and simpler, and significantly improves the segmentation performance.

3. Method

3.1. Overview

The overview of our proposed IFIRVOS is illustrated in Fig.2. It mainly consists of four parts: the image and text encoders, the vision-language interaction module, the multimodal Transformer with inter-frame interaction module and the instance sequence segmentation part. During inference, given a video sequence $\mathcal{V} = \{I_t\}_{t=1}^T$ with T frames and a referring expression of the target object $\mathcal{E} = \{e_l\}_{l=1}^L$ with L words, the image and text encoders first extract the multi-level visual features of the T frames and the word feature of the language expression, which are then fed into the vision-language interaction module to produce language-enhanced visual features and the sentence feature with decent correlation. The Transformer encoder takes the enhanced multi-level visual features as input and its outputs along with the sentence feature are submitted to the Transformer decoder, where the sentence feature serves as the language queries to decode the object information from the frame features and generates the instance embeddings. The inter-frame interaction module inserted in the Transformer decoder enables the instance embeddings for each frame with temporal coherence and spatio-temporal representation. Finally, the instance sequence segmentation part integrates the instance embeddings and the visual features to predict accurate segmentation sequence for referred object.

3.2. Feature Extraction

Image Encoder. For the frames in the video sequence, we adopt the image encoder to extract the multi-level visual features of each frame independently and obtain the visual feature sequence $F_v = \{f_t\}_{t=1}^T$, where f_t denotes the multi-level features for the t -th frame. Specifically, f_t is a four-level pyramid features, in which the first three-level features are the last three stage features of the image encoder with spatial strides of $\{8, 16, 32\}$, and the last-level feature is obtained by downsampling the 32-stride feature using a convolutional layer with stride 2, thus f_t is the four-level pyramid features with strides of $\{8, 16, 32, 64\}$.

Text Encoder. The linguistic feature are extracted from the language expression using the off-the-shelf text encoder, called RoBERTa [18]. Different from ReferFormer that generate both the word-level text feature (text feature) and the sentence-level feature (sentence feature), we only need the word feature $F_l \in R^{L \times C}$, which contains the feature embedding of each word in the language expression and has the same length L as the number of words in the language expression. Since the text feature is semantically rich and includes more object information, it is more suitable to perform fine-grained level cross-modal interaction with visual features to generate vision-enhanced text feature.

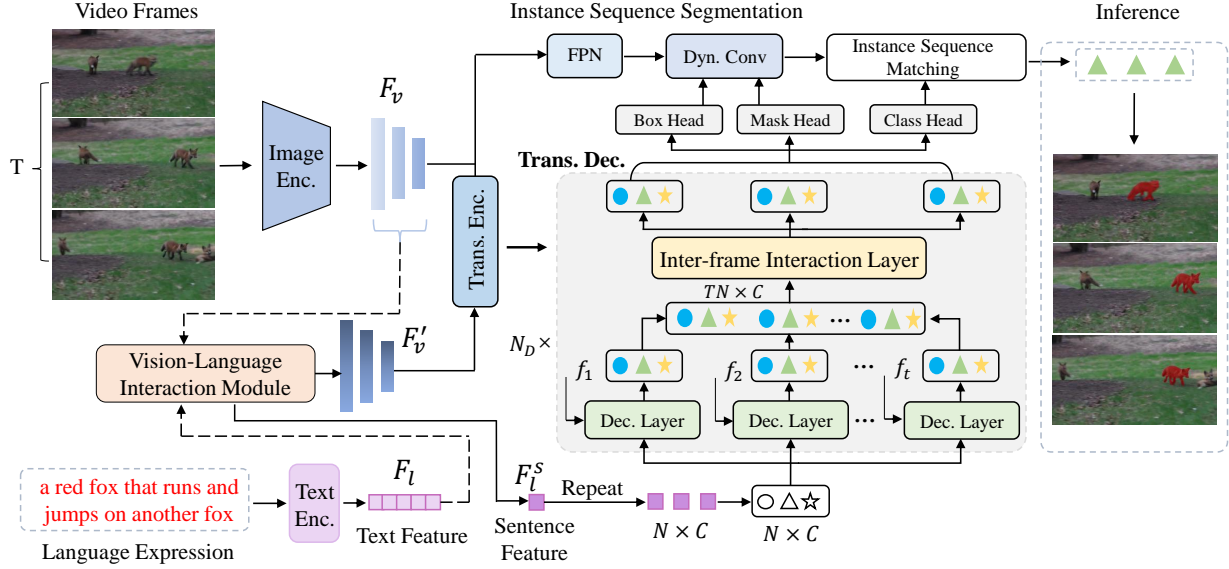


Figure 2. The overview of the proposed IFIRVOS method. It mainly consists of four parts: the image and text encoders, the vision-language interaction module, the multimodal Transformer with inter-frame interaction module and the instance sequence segmentation part. The vision-language interaction module constructs the correlation between the visual and linguistic features before they are sent into the multimodal Transformer. The inter-frame interaction module in the Transformer decoder enables the instance embeddings for each frame with temporal coherence and spatio-temporal representation. Here the same colors and shapes in the queries refer to the same object in different frames.

3.3. Vision-Language Interaction Module

As the task of RVOS involves segmenting a specified object in a given video sequence based on a language expression, how to align the cross-modal features and transfer the semantics from the language modality to the visual modality to help locate and segment the target object is important for this task.

The typical ReferFormer method proposes to use the sentence feature of the language expression as the queries to iteratively interact the visual features in the Transformer decoder and generate instance embeddings containing representation information of the referred object. However, the raw sentence feature is abstract and contains only high-level semantic information, and its correlation with the visual features is also weak because they have not interacted closely before the Transformer. We argue that the weak correlation between abstract sentence feature and the visual features will increase the difficulty of decoding the object information accurately in the Transformer decoder and finally limit the model performance.

Therefore, in this paper, we devise the *vision-language interaction module* to reinforce the cross-modal correlation between the visual and text features, and put it before the multimodal Transformer. As shown in Fig.3, the vision-language interaction module is composed of two parallel submodules, namely Vision Enhancement with Language

(VEwL) submodule and Language Enhancement with Vision (LEwV) submodule. Both submodules take the raw text feature F_l and multi-level visual feature sequence F_v as input, and the VEwL submodule outputs the language-enhanced multi-level visual features F'_v while the LEwV submodule produces the vision-enhanced sentence feature F_l^s . We will describe these two submodules in detail in the following part.

Language Enhancement with Vision submodule starts with a cross-modal interaction between text feature and visual features, where the visual features serve as the guidance to enhance the text feature. As shown in Fig.3, the raw text feature F_l and the original multi-level visual feature sequence F_v are the input of the LEwV submodule, which is composed of a multi-head attention layer and a multiplier layer [38]. LEwV submodule iteratively processes the text feature and the single-level visual feature sequence for N_l times until the text feature interacts with all levels of visual feature sequence. N_l is the number of levels of the multi-level visual feature sequence F_v .

The multi-head attention layer adopts the cross-attention mechanism to accomplish the cross-modal interaction between the text feature and visual features, where the text feature $F_l \in R^{L \times C}$ serves as the query (Q) and the single-level visual features $F_v^i \in R^{H_i \times W_i \times C}$ is used as the key-value pair (K-V). Here H_i and W_i are the height and width of the i -th level of features, and C is the channel number.

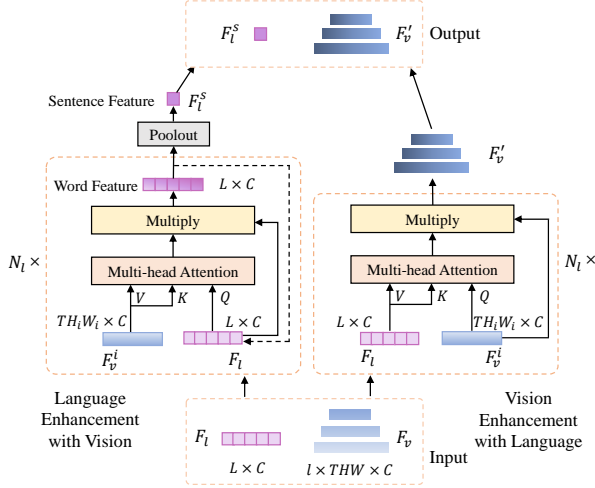


Figure 3. The structure of the vision-language interaction module.

For simplicity, we present the cross-attention based cross-modal interaction process in a single-head manner. For the i -th iteration, the attention layer first obtains the cross-modal similarity matrix $A_{vl}^i \in R^{L \times TH_i W_i}$ by computing the similarity between each word embedding and each pixel embedding as follows:

$$A_{vl}^i = \text{Softmax}\left(\frac{F_l^i W^Q \cdot (F_v^i W^K)^T}{\sqrt{d_k}}\right), \quad (1)$$

where $W^Q, W^K \in R^{C \times d_k}$ are learnable linear projections. Then we use A_{vl}^i to aggregate the language-related target information in the visual features and multiply with the input text feature F_l^i to obtain the vision-enhanced text feature F_l^{i+1} :

$$F_l^{i+1} = (A_{vl}^i F_v^i W^V) \cdot F_l^i, \quad (2)$$

where W^V is the learnable linear projection. To obtain positional information, a fixed two-dimensional sinusoidal positional encoding is added to the visual features before the cross-attention process. The raw text feature F_l is F_l^0 in the first iteration.

After the last iteration of the cross-modal interaction, the final vision-enhanced text feature F_l^s is converted to vision-enhanced sentence feature $F_l^s \in \mathbb{R}^C$ by performing the poolout operation in the RoBERTa model.

Vision Enhancement with Language submodule has the same submodule architecture and input features with the LEwV submodule, as shown in Fig.3. However, the VEwL submodule has different running procedure. Each level of the original multi-level visual feature sequence F_v interacts with the raw text feature F_l individually via the multi-head attention layer and the multiplier layer. Similarly, for each cross-modal interaction, the multi-head attention layer performs the cross-attention on the text feature

F_l and the single-level visual feature sequence F_v^i , where the visual features act as the query (Q) and the text feature serves as the key-value pair (K-V). The attention layer first derives the cross-modal similarity matrix $A_{vl}^i \in R^{TH_i W_i \times L}$ by computing the similarity between each pixel embedding and each word embedding as follows:

$$A_{vl}^i = \text{Softmax}\left(\frac{F_v^i W^Q \cdot (F_l W^K)^T}{\sqrt{d_k}}\right), \quad (3)$$

where $W^Q, W^K \in R^{C \times d_k}$ are learnable linear projections. Then the similarity matrix is used to aggregate the vision-related object information in the text features followed by the multiplication with the input visual feature F_v^i to obtain the language-enhanced single-level visual feature $F_v^{i'}$

$$F_v^{i'} = A_{vl}^i F_l W^V \cdot F_v^i, \quad (4)$$

where W^V is the learnable linear projection. To obtain positional information, we add fixed one-dimensional sinusoidal positional encoding to the text feature before the cross-attention operation.

After the cross-modal interaction of each level of the multi-level visual feature sequence F_v with the raw text features F_l , we obtain the language-enhanced multi-level visual feature sequence $F_v^{i'}$.

3.4. Multimodal Transformer

The multimodal Transformer aims to exploit the vision-enhanced sentence feature and the language-enhanced multi-level visual feature sequence to produce the target-aware instance embeddings, which are converted to conditional convolution kernels to perform conditional convolution [29] on the visual features and generate the final segmentation masks. Here we adopt the Deformable-DETR [42] as the multimodal Transformer like [35] and use the vision-enhanced sentence feature F_l^s as the language queries of the decoder to find the referred object.

Transformer Encoder. Before feeding the language-enhanced multi-level visual features into the Transformer encoder, the fixed 2D positional encodings are added to the feature maps of each frame to reinforce the position information. After that, the multi-level features are processed by the encoder in a frame-independent manner and the output features are fed into the decoder. Besides, the first three stage features of Transformer encoder output and the backbone feature with spatial stride of 4 are sent together into the cross-modal FPN [35] to generate the final feature maps for segmentation, *i.e.*, $F_{seg} = \{f_{seg}^t\}_{t=1}^T$, where $f_{seg}^t \in \mathbb{R}^{\frac{H}{4} \times \frac{W}{4} \times C}$, H and W are the height and width of the input frames.

Transformer Decoder. As shown in Fig.2, to enhance the feature learning ability of the decoder, we repeat the sentence feature for N times to generate N object queries

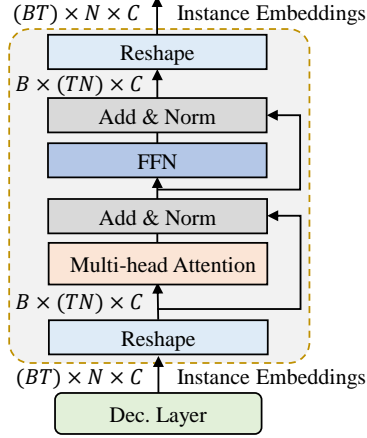


Figure 4. The architecture of the inter-frame interaction layer of the inter-frame interaction module.

for each frame as in [35]. The encoder output, the language queries, and the learnable reference point embeddings as in Deformable-DETR are fed into the decoder. Then, the language queries interact with the visual feature and try to find the referred object only, resulting in the set of $N_q = T \times N$ instance embeddings.

Similar with [35], the decoding process of the language queries and the visual features is implemented in a frame-independent fashion, which however leads to a lack of inter-frame communication between the instance embeddings generated for each frame and the absence of temporal coherence of the target object, and affects the final segmentation performance. To address this issue and introduce the spatio-temporal representation for the instance embeddings, we propose the inter-frame interaction module that enables the instance embeddings of each frame to make good use of the temporal information between frames, allowing for better tracking and segmentation of the referred object in the video sequence.

Inter-frame Interaction Module is a plug-and-play module for the Transformer decoder. The module contains several inter-frame interaction layer, each of which is inserted behind each decoder layer in the Transformer to efficiently model the temporal coherence and learn the spatio-temporal representation for the instance embeddings, as shown in Fig.4. Specifically, the instance embeddings $Q \in R^{(BT) \times N \times C}$ generated by the frame-independent decoding process are first unfolded in the spatio-temporal dimension to obtain $Q \in R^{B \times (TN) \times C}$. Here B is the batch size. Then, instance embeddings Q are fed into the standard multi-head self-attention layer [30] and the feed-forward network (FFN), where the inter-frame global correlation are constructed and spatio-temporal representation of the queried object are learned. The instance embeddings output from the inter-frame interaction layer are transformed back

into the frame-independent state, *i.e.*, $Q \in R^{(BT) \times N \times C}$, and then sent to the next decoder layer or directly as the output of the decoder. The inter-frame interaction layer could be formulated as follows:

$$\begin{aligned} Q_1 &= LN(Atten(Re(Q)) + Re(Q)), \\ Q_2 &= Re(LN(FFN(Q_1) + Q_1)), \end{aligned} \quad (5)$$

where $Re(\cdot)$ represents the reshape operation, $Atten(\cdot)$ represents the multi-head attention layer, $LN(\cdot)$ denotes the layer normalization, and $FFN(\cdot)$ denotes the feed-forward network.

3.5. Instance Sequence Segmentation

As shown in 2, three prediction heads are built on top of the decoder to further transform the N_q instance embeddings from the decoder, *i.e.*, box head, mask head, and class head. The class head predicts whether the predicted instance is described by the expression or whether the instance is available in the current frame. The mask head consists of three linear layers and is responsible for predicting the parameters of the conditional convolution kernels $\Omega = \{\omega_i\}_{i=1}^{N_q}$, which are reshaped to form three 1×1 convolution kernels. The box head is a 3-layer feed-forward network with ReLU activation except for the last layer. It predicts the box location of the referred object. Finally, we implement the instance sequence segmentation and produce the final frame-order mask sequence predictions $S \in R^{T \times N \times \frac{W}{4} \times \frac{H}{4}}$ by applying the conditional convolution kernels $\Omega = \{\omega_i\}_{i=1}^{N_q}$ on the corresponding feature maps, which are the concatenation of the feature maps F_{seg} and relative box coordinates as [35] did.

During the training process, the predicted instance sequence is treated as a whole and supervised by the instance matching strategy [32]. We denote the instance prediction sequences as $\hat{y} = \{\hat{y}_i\}_{i=1}^N$, and the predictions for the i -th instance is denoted as:

$$\hat{y}_i = \left\{ \hat{p}_i^t, \hat{b}_i^t, \hat{s}_i^t \right\}_{t=1}^T, \quad (6)$$

where $\hat{p}_i^t \in R^1$ is the probability score predicted by the class head for the t -th frame in the video sequence. $\hat{b}_i^t \in R^4$ is the normalized coordinates that defines the center point as well as the height and width of the prediction box. $\hat{s}_i^t \in R^{\frac{H}{4} \times \frac{W}{4}}$ is the predicted binary segmentation mask.

The ground truth instance sequence could be represented as $y = \{c^t, b^t, s^t\}_{t=1}^T$, where c^t is an one-hot value that equals 1 when the ground truth instance is visible in the t -th frame and 0 otherwise. b^t and s^t are the corresponding normalized box coordinates and segmentation mask. To train the network, we first locate the best prediction sequence from all the instance prediction sequences as the positive

sample by minimizing the following matching cost:

$$\hat{y}_{\text{pos}} = \arg \min_{\hat{y}_i \in \hat{\mathcal{Y}}} \mathcal{L}_{\text{match}}(y, \hat{y}_i), \quad (7)$$

where

$$\begin{aligned} \mathcal{L}_{\text{match}}(y, \hat{y}_i) = & \lambda_{\text{cls}} \mathcal{L}_{\text{cls}}(c, \hat{p}_i) + \lambda_{\text{box}} \mathcal{L}_{\text{box}}(b, \hat{b}_i) \\ & + \lambda_{\text{mask}} \mathcal{L}_{\text{mask}}(s, \hat{s}_i), \end{aligned} \quad (8)$$

here, \mathcal{L}_{cls} is the focal loss [16], \mathcal{L}_{cls} is the sum of the L1 loss and GIoU loss, and $\mathcal{L}_{\text{mask}}$ is the combination of DICE loss [24] and binary mask focal loss. The matching cost is calculated from each frame and normalized by the frames number. Then the whole model is optimized by minimizing the matching loss of the positive sample.

During inference, given a video sequence and the language expression, IFIRVOS could predict N instance sequences corresponding to the N queries. For each prediction sequence, we average the predicted class probabilities over all the frames and get the probability score set $P = \{p_i\}_{i=1}^N$, and we select the sequence with the highest score as the final predictions of the input video sequence without any post-process technique.

4. Experiences

4.1. Datasets and Metrics

Datasets. The experiments are conducted on the three popular RVOS benchmarks: Ref-Youtube-VOS [28], Ref-DAVIS17 [12], and A2D-Sentences [7]. Ref-Youtube-VOS is a large-scale benchmark which covers 3471 videos with 12913 expressions in the training set and 202 videos with 2096 expressions in the validation set. Ref-DAVIS17 is split into 60 videos and 30 videos for training and validation, respectively. We only use the validation set for evaluation. A2D-Sentences is created by providing the additional textual annotations on the original A2D dataset [36].

Evaluation Metrics. Following the standard evaluation protocol [28], we use the region similarity J , contour accuracy F , and their average value $J\&F$ for the evaluation on the Ref-Youtube-VOS and Ref-DAVIS17. Since there is no publicly available ground truth annotations of the Ref-Youtube-VOS val set, we submit our predictions to the official server to get the evaluation results. For A2D-Sentences, the model is evaluated in the metrics of Precision@K, Overall IoU, Mean IoU and mAP over 0.50:0.05:0.95 like [35].

4.2. Implementation Details

Model Settings. Due to the limitation of our GPU (RTX 3090 for ours *vs* V100 for ReferFormer [35]), we can only use the ResNet50 [8] pre-trained on ImageNet [5] as the image encoders for training and inference and realize a

Method	Backbone	$J\&F$	J	F
URVOS [28]	ResNet-50	47.2	45.3	49.2
YOFO [13]	ResNet-50	48.6	47.5	49.7
LBSTI [6]	ResNet-50	49.4	48.2	50.6
MLSA [34]	ResNet-50	49.7	48.4	51.0
MTTR [2]	Video-Swin-T	55.3	54.0	56.6
ReferFormer [35]	ResNet-50	55.6	54.8	56.5
CITD [15]	ResNet-101	56.4	54.8	58.1
ReferFormer [35]	ResNet-101	57.3	56.1	58.4
ReferFormer [35]	Video-Swin-T	59.4	58.0	60.9
IFIRVOS	ResNet-50	59.9	58.4	61.4

Table 1. Comparison with state-of-the-art methods on the Ref-Youtube-VOS val set.

Method	Backbone	$J\&F$	J	F
CMSA+RNN [39]	ResNet-50	40.2	36.9	43.5
URVOS [28]	ResNet-50	51.6	47.3	56.0
MLSA* [34]	ResNet-50	52.7	50.0	55.4
LBSTI [6]	ResNet-50	54.3	-	-
MLSA [34]	ResNet-50	57.9	53.9	62.0
ReferFormer* [35]	ResNet-50	58.5	55.8	61.3
IFIRVOS*	ResNet-50	60.5	56.9	64.1

Table 2. Comparison with state-of-the-art methods on the Ref-DAVIS17 val set. * means no fine-tuning on the Ref-DAVIS17 training set.

fair comparison with ReferFormer [35]. For the Multimodal Transformer, we adopt 4 encoder layers and 4 decoder layers with the hidden dimension $C = 256$. The number of language queries N is set as 5 and the number of the levels of the multi-level visual features N_l is 4.

Training Details. The training of our model is divided into two stages as [35]. We first pre-train our model on the RIS datasets, including Ref-COCO [41], Ref-COCOg [41], and Ref-COCO+ [22], with the number of frames $T = 1$ and a batch size of 2 on each GPU. The model is pre-train for 10 epochs with the learning rate reduced by a factor of 0.1 at the 6th and 8th epochs. After the pre-training stage, we employ different fine-tuning strategies to tune the model on different RVOS validation sets. For the Ref-Youtube-VOS and Ref-DAVIS17 datasets, we fine-tune the pre-trained model on Ref-Youtube-VOS training set with 1 video sequence per GPU for 6 epochs, where the learning rate is reduced by a factor of 0.1 at the 3th and 5th epoch, respectively. Each video sequence consists of 6 randomly sampled frames from the same video with data augmentations applied, including random horizontal flip, random crop, and photometric distortion. All input frames are re-

Method	Backbone	Precision					IoU		mAP
		P@0.5	P@0.6	P@0.7	P@0.8	P@0.9	Overall	Mean	
ACAN [31]	I3D	55.7	45.9	31.9	16.0	2.0	60.1	49.0	27.4
CSTM [10]	I3D	65.4	58.9	49.7	33.3	9.1	66.2	56.1	39.9
CMPC-V [17]	I3D	65.5	59.2	50.6	34.2	9.8	65.3	57.3	40.4
MTTR [2]	Video-Swin-T	72.1	68.4	60.7	45.6	16.4	70.2	61.8	44.7
LBSTI [6]	ResNet-50	73.0	67.4	59.0	42.1	13.2	70.4	62.1	47.2
ClawCraneNet [14]	ResNet-50	70.4	67.7	61.7	48.9	17.1	63.1	59.9	49.4
ReferFormer [35]	ResNet-50	78.9	75.7	68.7	51.5	17.6	74.5	66.5	51.1
IFIRVOS	ResNet-50	80.0	77.2	70.2	53.6	19.8	74.7	67.6	52.4

Table 3. Comparison with state-of-the-art methods on the A2D-Sentences.

sized to have a short side of 360 and the maximum long side of 640. The model is optimized using the AdamW optimizer [20] with the initial learning rate of 1×10^{-5} for the image and text encoders, and 5×10^{-5} for the rest parts. It should be noted that the text encoder is optimized during the pre-training phase while its parameters are frozen during the fine-tuning process. For A2D-Sentences, we fine-tune the pre-trained model on the A2D-Sentences training set with the same setting as Ref-Youtube-VOS. The loss weights for different losses are set as $\lambda_{cls} = 2$, $\lambda_{L1} = 5$, $\lambda_{giou} = 2$, $\lambda_{dice} = 1$, and $\lambda_{focal} = 1$.

4.3. Comparison with State-of-the-Art Methods

Ref-Youtube-VOS val set. We compare our method with several state-of-the-art approaches on the Ref-Youtube-VOS val set and the results are reported in Table ?? . It can be observed that our IFIRVOS achieves the overall $J&F$ accuracy of 59.9% on the Ref-Youtube-VOS val set, which outperforms the previous methods, such as LBSTI [6], MLSA [34] and CITD [15], with a large margin. Particularly, compared with the ReferFormer with the same ResNet-50 backbone, our IFIRVOS is 4.3% higher than it at the $J&F$ accuracy, and even surpasses the ReferFormer with stronger ResNet-101 [8] and Video-Swin-Tiny [19] backbones by 2.6% and 0.5%, respectively. These results validate the effectiveness of our proposed IFIRVOS for RVOS task and demonstrate that our method achieves state-of-the-art performance.

Ref-DAVIS17 val set. We further evaluate the performance of our proposed model on the Ref-DAVIS17 val set. The results are summarized in Table ?? . Following the setting in ReferFormer, we directly report the evaluation results using the model trained on the Ref-Youtube-VOS training set, which means the model is not fine-tuned on the Ref-DAVIS17 dataset. As we can see, our approach realizes the overall $J&F$ accuracy of 60.5%, which exceeds all the comparison methods and is 2.0% higher than the state-of-the-art ReferFormer with the same backbone.

Moreover, compared with the methods that are fine-tuned on the Ref-DAVIS17 dataset, *e.g.*, URVOS [28], LBSTI [6] and MLSA [34], our model, without fine-tuning on the target dataset, also outperforms them by a large margin, *e.g.*, 8.9% higher than URVOS, 6.2% higher than LBSTI and 2.6% higher than MLSA, which shows the good generalization of our model. These results further validate the effectiveness of introducing the inter-frame interaction mechanism and the cross-modal correlation in the decoder for solving RVOS task.

A2D-Sentences test set. We also evaluate the performance of the proposed IFIRVOS on the A2D-Sentences test set and compare it with other cutting-edge methods. The results are presented in Table ?? . It can be observed that our approach achieves 52.4 mAP and outperforms all the cutting-edge methods. Concretely, compared with the models using the powerful spatial-temporal backbones, our model delivers better results, *e.g.*, a gain of 12.0 mAP over CMPC-V [17] with the I3D backbone and 7.7 mAP over MTTR [2] using the Video-Swin-T. For the methods with the same ResNet-50 backbone, *e.g.*, ClawCraneNet [14] and ReferFormer [35], IFIRVOS surpasses it in all metrics.

Fig.5 presents the visualization comparison between ReferFormer and IFIRVOS, and we intuitively observe that our IFIRVOS outperforms the ReferFormer in terms of the accuracy and consistency between frames of prediction results.

4.4. Model analysis

In this part, we perform extensive ablation experiments to investigate the influence of the core components of our IFIRVOS as well as the impact of different model settings. All of the experiments are conducted on the Ref-Youtube-VOS dataset.

Components Analysis. To explore the influence of the key components of our model, we first build a baseline model which is the IFIRVOS without the inter-frame interaction module and the vision-language interaction module.

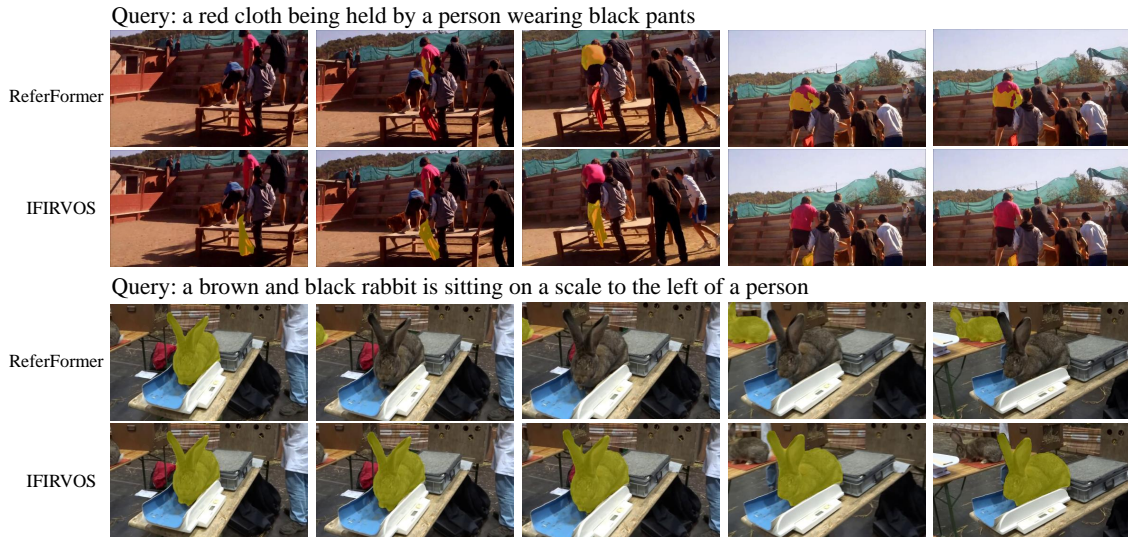


Figure 5. Visualization comparison between ReferFormer and IFIRVOS.

Method	IFI	VLI	$J\&F$	\mathcal{J}	\mathcal{F}
Baseline			55.1	54.0	56.2
IFIRVOS		✓	57.1	55.9	58.3
IFIRVOS	✓		58.8	57.4	60.2
IFIRVOS	✓	✓	59.9	58.4	61.4

Table 4. Ablation study of different components of the proposed IFIRVOS on Ref-Youtube-VOS *val* set. IFI denotes inter-frame interaction module, and VLI denotes vision-language interaction module.

As shown in Table ??, the baseline model obtains an overall $J\&F$ accuracy of 55.1%. When we add the vision-language interaction module on the baseline model, the special IFIRVOS achieves an overall $J\&F$ accuracy of 57.1%, which is 2.0% higher than the baseline. The improvement proves the effectiveness of the vision-language interaction module. When only the inter-frame interaction module is imposed on the baseline, the $J\&F$ accuracy of the special IFIRVOS reaches to 58.8%, which means the module brings a 3.7% gain and validates the superiority of the module. Equipped with both components, our IFIRVOS can achieve the best performance.

Vision-Language Interaction Module. In this study, we explore the impact of different settings in the vision-language interaction module. The first is the interaction strategy between visual and text features. We design two types of interaction settings, i.e., 'Attention + Multiply', and 'Attention + FFN'. The former setting is adopted in IFIRVOS and the later is a common paradigm. The exper-

Method	Settings	$J\&F$	\mathcal{J}	\mathcal{F}
Interaction Strategies				
IFIRVOS	Attention+Multiply	59.9	58.4	61.4
IFIRVOS	Attention+FFN	58.7	57.4	60.1
Interaction Procedure of VEWL submodule				
IFIRVOS	Fixed	59.9	58.4	61.4
IFIRVOS	Dynamic	58.0	56.7	59.3

Table 5. Model analysis of different settings in the vision-language interaction module.

imental results are reported in Table ?. It can be seen that the IFIRVOS with the default setting performs better than the one with the later setting, which means that the 'Attention + Multiply' strategy may be more suitable for cross-modal interaction.

The second setting is the interaction procedure of the VEWL submodule. In our model, we use the *fixed* raw text feature to interact with each level of the multi-level visual features. Here we study the another interaction procedure that the next level of the visual feature is interacted with the *dynamically* updated text feature from the last cross-modal interaction. The results are presented in Table ?. It can be observed that IFIRVOS with the *fixed* text feature setting outperforms the one with dynamical text feature setting by about 2% $J\&F$ accuracy. The reason may be that the essential information in the raw text feature is not corrupted by the iterative interaction processes, thus making it more suitable for the cross-modal interaction with visual features.

5. Conclusion

In this paper, we propose a novel RVOS framework, termed IFIRVOS, to solve the issues of inter-frame interaction and cross-modal correlation in the decoding process of the language queries based RVOS methods. We design the plug-and-play inter-frame interaction module for the Transformer decoder to efficiently model the temporal coherence and learn the spatio-temporal representation of the referred object, so as to decode the object information in the video sequence more precisely and generate more accurate segmentation results. Moreover, we devise the vision-language interaction module and place it before the Transformer to enhance the correlation between the visual and linguistic features, thus facilitating the process of decoding object information from visual features using language queries in the Transformer decoder and improving the performance. Experimental results on three benchmark datasets validate the superiority of our IFIRVOS over state-of-the-art methods and the effectiveness of our proposed modules.

References

- [1] Miriam Bellver, Carles Ventura, Carina Silberer, Ioannis Kazakos, Jordi Torres, and Xavier Giro-i Nieto. Refvos: A closer look at referring expressions for video object segmentation. *arXiv preprint arXiv:2010.00263*, 2020.
- [2] Adam Botach, Evgenii Zheltonozhskii, and Chaim Baskin. End-to-end referring video object segmentation with multi-modal transformers. In *CVPR*, pages 4985–4995, 2022.
- [3] Nicolas Carion, Francisco Massa, Gabriel Synnaeve, Nicolas Usunier, Alexander Kirillov, and Sergey Zagoruyko. End-to-end object detection with transformers. In *ECCV*, pages 213–229, 2020.
- [4] Bowen Cheng, Ishan Misra, Alexander G Schwing, Alexander Kirillov, and Rohit Girdhar. Masked-attention mask transformer for universal image segmentation. In *CVPR*, pages 1290–1299, 2022.
- [5] Jia Deng, Wei Dong, Richard Socher, Li-Jia Li, Kai Li, and Li Fei-Fei. Imagenet: A large-scale hierarchical image database. In *CVPR*, pages 248–255, 2009.
- [6] Zihan Ding, Tianrui Hui, Junshi Huang, Xiaoming Wei, Jizhong Han, and Si Liu. Language-bridged spatial-temporal interaction for referring video object segmentation. In *CVPR*, pages 4964–4973, 2022.
- [7] Kirill Gavrilyuk, Amir Ghodrati, Zhenyang Li, and Cees GM Snoek. Actor and action video segmentation from a sentence. In *CVPR*, pages 5958–5966, 2018.
- [8] Kaiming He, Xiangyu Zhang, Shaoqing Ren, and Jian Sun. Deep residual learning for image recognition. In *CVPR*, pages 770–778, 2016.
- [9] Miran Heo, Sukjun Hwang, Seoung Wug Oh, Joon-Young Lee, and Seon Joo Kim. Vita: Video instance segmentation via object token association. In *NIPS*, 2022.
- [10] Tianrui Hui, Shaofei Huang, Si Liu, Zihan Ding, Guanbin Li, Wenguan Wang, Jizhong Han, and Fei Wang. Collaborative spatial-temporal modeling for language-queried video actor segmentation. In *CVPR*, pages 4187–4196, 2021.
- [11] Sukjun Hwang, Miran Heo, Seoung Wug Oh, and Seon Joo Kim. Video instance segmentation using inter-frame communication transformers. In *NIPS*, pages 13352–13363, 2021.
- [12] Anna Khoreva, Anna Rohrbach, and Bernt Schiele. Video object segmentation with language referring expressions. In *ACCV*, pages 123–141. Springer, 2018.
- [13] Dezhuang Li, Ruoqi Li, Lijun Wang, Yifan Wang, Jinqing Qi, Lu Zhang, Ting Liu, Qingquan Xu, and Huchuan Lu. You only infer once: Cross-modal meta-transfer for referring video object segmentation. In *AAAI*, pages 1297–1305, 2022.
- [14] Chen Liang, Yu Wu, Yawei Luo, and Yi Yang. Clawcranenet: Leveraging object-level relation for text-based video segmentation. *arXiv preprint arXiv:2103.10702*, 2021.
- [15] Chen Liang, Yu Wu, Tianfei Zhou, Wenguan Wang, Zongxin Yang, Yunchao Wei, and Yi Yang. Rethinking cross-modal interaction from a top-down perspective for referring video object segmentation. *arXiv preprint arXiv:2106.01061*, 2021.
- [16] Tsung-Yi Lin, Priya Goyal, Ross Girshick, Kaiming He, and Piotr Dollár. Focal loss for dense object detection. In *ICCV*, pages 2980–2988, 2017.
- [17] Si Liu, Tianrui Hui, Shaofei Huang, Yunchao Wei, Bo Li, and Guanbin Li. Cross-modal progressive comprehension for referring segmentation. *TPAMI*, 2021.
- [18] Yinhan Liu, Myle Ott, Naman Goyal, Jingfei Du, Mandar Joshi, Danqi Chen, Omer Levy, Mike Lewis, Luke Zettlemoyer, and Veselin Stoyanov. Roberta: A robustly optimized bert pretraining approach. *arXiv preprint arXiv:1907.11692*, 2019.
- [19] Ze Liu, Jia Ning, Yue Cao, Yixuan Wei, Zheng Zhang, Stephen Lin, and Han Hu. Video swin transformer. In *CVPR*, pages 3202–3211, 2022.
- [20] Ilya Loshchilov and Frank Hutter. Decoupled weight decay regularization. In *ICLR*, 2018.
- [21] Xiankai Lu, Wenguan Wang, Danelljan Martin, Tianfei Zhou, Jianbing Shen, and Van Gool Luc. Video object segmentation with episodic graph memory networks. In *ECCV*, pages 661–679, 2020.
- [22] Junhua Mao, Jonathan Huang, Alexander Toshev, Oana Camburu, Alan L Yuille, and Kevin Murphy. Generation and comprehension of unambiguous object descriptions. In *CVPR*, pages 11–20, 2016.
- [23] Bruce McIntosh, Kevin Duarte, Yogesh S Rawat, and Mubarak Shah. Visual-textual capsule routing for text-based video segmentation. In *CVPR*, pages 9942–9951, 2020.
- [24] Fausto Milletari, Nassir Navab, and Seyed-Ahmad Ahmadi. V-net: Fully convolutional neural networks for volumetric medical image segmentation. In *2016 fourth international conference on 3D vision (3DV)*, pages 565–571, 2016.
- [25] Federico Perazzi, Jordi Pont-Tuset, Brian McWilliams, Luc Van Gool, Markus Gross, and Alexander Sorkine-Hornung. A benchmark dataset and evaluation methodology for video object segmentation. In *CVPR*, pages 724–732, 2016.

- [26] Jordi Pont-Tuset, Federico Perazzi, Sergi Caelles, Pablo Arbelaez, Alexander Sorkine-Hornung, and Luc Van Gool. The 2017 DAVIS challenge on video object segmentation. *abs/1704.00675*, 2017.
- [27] Zheyun Qin, Xiankai Lu, Xiushan Nie, Xiantong Zhen, and Yilong Yin. Learning hierarchical embedding for video instance segmentation. In *ACMMM*, pages 1884–1892, 2021.
- [28] Seonguk Seo, Joon-Young Lee, and Bohyung Han. Urvos: Unified referring video object segmentation network with a large-scale benchmark. In *ECCV*, pages 208–223. Springer, 2020.
- [29] Zhi Tian, Chunhua Shen, and Hao Chen. Conditional convolutions for instance segmentation. In *ECCV*, pages 282–298, 2020.
- [30] Ashish Vaswani, Noam Shazeer, Niki Parmar, Jakob Uszkoreit, Llion Jones, Aidan N. Gomez, Lukasz Kaiser, and Illia Polosukhin. Attention is all you need. In *NIPS*, pages 5998–6008, 2017.
- [31] Hao Wang, Cheng Deng, Junchi Yan, and Dacheng Tao. Asymmetric cross-guided attention network for actor and action video segmentation from natural language query. In *ICCV*, pages 3939–3948, 2019.
- [32] Yuqing Wang, Zhaoliang Xu, Xinlong Wang, Chunhua Shen, Baoshan Cheng, Hao Shen, and Huaxia Xia. End-to-end video instance segmentation with transformers. In *CVPR*, pages 8741–8750, 2021.
- [33] Zhaoqing Wang, Yu Lu, Qiang Li, Xunqiang Tao, Yandong Guo, Mingming Gong, and Tongliang Liu. Cris: Clip-driven referring image segmentation. In *CVPR*, pages 11686–11695, 2022.
- [34] Dongming Wu, Xingping Dong, Ling Shao, and Jianbing Shen. Multi-level representation learning with semantic alignment for referring video object segmentation. In *CVPR*, pages 4996–5005, 2022.
- [35] Jiannan Wu, Yi Jiang, Peize Sun, Zehuan Yuan, and Ping Luo. Language as queries for referring video object segmentation. In *CVPR*, pages 4974–4984, 2022.
- [36] Chenliang Xu, Shao-Hang Hsieh, Caiming Xiong, and Jason J Corso. Can humans fly? action understanding with multiple classes of actors. In *CVPR*, pages 2264–2273, 2015.
- [37] Ning Xu, Linjie Yang, Yuchen Fan, Jianchao Yang, Dingcheng Yue, Yuchen Liang, Brian L. Price, Scott Cohen, and Thomas S. Huang. Youtube-vos: Sequence-to-sequence video object segmentation. In *ECCV*, pages 603–619, 2018.
- [38] Zhao Yang, Jiaqi Wang, Yansong Tang, Kai Chen, Hengshuang Zhao, and Philip HS Torr. Lavt: Language-aware vision transformer for referring image segmentation. In *CVPR*, pages 18155–18165, 2022.
- [39] Linwei Ye, Mrigank Rochan, Zhi Liu, and Yang Wang. Cross-modal self-attention network for referring image segmentation. In *CVPR*, pages 10502–10511, 2019.
- [40] Licheng Yu, Zhe Lin, Xiaohui Shen, Jimei Yang, Xin Lu, Mohit Bansal, and Tamara L Berg. Mattnet: Modular attention network for referring expression comprehension. In *CVPR*, pages 1307–1315, 2018.
- [41] Licheng Yu, Patrick Poirson, Shan Yang, Alexander C Berg, and Tamara L Berg. Modeling context in referring expressions. In *ECCV*, pages 69–85, 2016.
- [42] Xizhou Zhu, Weijie Su, Lewei Lu, Bin Li, Xiaogang Wang, and Jifeng Dai. Deformable detr: Deformable transformers for end-to-end object detection. In *ICLR*, 2020.